NEUROPATHOLOGY

Reversal of endothelial dysfunction reduces white matter vulnerability in cerebral small vessel disease in rats

Rikesh M. Rajani[1], Sophie Quick[1], Silvie R. Ruigrok[1], Delyth Graham[2], Sarah E. Harris[3], Benjamin F. J. Verhaaren[4,5], Myriam Fornage[5,6], Sudha Seshadri[5,7], Santosh S. Atanur[8], Anna F. Dominiczak[2], Colin Smith[9], Joanna M. Wardlaw[10], Anna Williams[1]*

Dementia is a major social and economic problem for our aging population. One of the most common causes of dementia in the elderly is cerebral small vessel disease (SVD). Magnetic resonance scans of SVD patients typically show white matter abnormalities, but we do not understand the mechanistic pathological link between blood vessels and white matter myelin damage. Hypertension is suggested as the cause of sporadic SVD, but a recent alternative hypothesis invokes dysfunction of the blood-brain barrier as the primary cause. In a rat model of SVD, we show that endothelial cell (EC) dysfunction is the first change in development of the disease. Dysfunctional ECs secrete heat shock protein 90α, which blocks oligodendroglial differentiation, contributing to impaired myelination. Treatment with EC-stabilizing drugs reversed these EC and oligodendroglial pathologies in the rat model. EC and oligodendroglial dysfunction were also observed in humans with early, asymptomatic SVD pathology. We identified a loss-of-function mutation in ATPase11B, which caused the EC dysfunction in the rat SVD model, and a single-nucleotide polymorphism in ATPase11B that was associated with white matter abnormalities in humans with SVD. We show that EC dysfunction is a cause of SVD white matter vulnerability and provide a therapeutic strategy to treat and reverse SVD in the rat model, which may also be of relevance to human SVD.

INTRODUCTION

One of the biggest challenges currently facing society is the increasing number of people with dementia as the population ages. Cerebral small vessel disease (SVD) affects the small perforating arterioles in the brain and is the leading cause of vascular dementia (*1*, *2*). SVD also contributes to and worsens the symptoms of Alzheimer's disease (*2*) and is responsible for up to 45% of dementias. Monogenic forms and some sporadic cases of SVD occur at young ages, which supports SVD as a disease rather than simply being a consequence of aging (*3*). In addition to dementia, SVD causes cognitive impairment, gait and balance problems (*2*, *4*, *5*), and trebles the risk of stroke (*6*). Its diagnosis relies on clinical presentation of lacunar stroke or cognitive or gait/balance problems with magnetic resonance imaging (MRI) features such as white matter hyperintensities (WMH) (*7*). These WMH are associated with cognitive decline in SVD (*6*), and pathological diagnosis of SVD relies on characteristic changes such as lipohyalinosis (asymmetric areas of small vessel fibrosis associated with foam cells and leakage of plasma proteins) and myelin loss (*8*), indicating that white matter damage plays an important role in disease pathogenesis.

The risk of sporadic SVD is increased by typical vascular risk factors such as hypertension, diabetes, and smoking (*9*–*11*). Despite one-third of people over the age of 80 having some signs of SVD (*12*), there are currently no established SVD therapies (*13*). Most treatments tested in clinical trials so far have focused on blood pressure reduction (*13*), although 30% of SVD patients are normotensive (*14*). Alternatively, some evidence now suggests that blood-brain barrier (BBB) changes may cause SVD (*15*, *16*). The BBB prevents unwanted cells and solutes in the blood from entering the brain parenchyma and is made of endothelial cells (ECs), pericytes, astrocyte end feet, and junctions between these cells (*17*). Disruption of the BBB is found in SVD (*16*, *18*), but it is unclear whether this causes any observed pathological changes or is secondary to them.

We sought mechanisms linking vascular changes with white matter pathology by studying the earliest pathological features of SVD in a rat model and human tissue. We show that the first pathological change is EC dysfunction, which occurs before the onset of hypertension or clinical signs. We identify both an upstream genetic cause of this EC dysfunction and a secreted downstream effector affecting the surrounding white matter. We also show that drug treatment to stabilize EC dysfunction in a SVD model reverses the endothelial and oligodendroglial pathologies, suggesting a new therapeutic strategy.

RESULTS

To study the early changes in SVD development, we used the stroke-prone spontaneously hypertensive rat [SHRSP; subsequently referred to as disease model (DM)]. This is an inbred rat strain known to be a relevant rodent model of human sporadic SVD (*19*, *20*). These

[1]Medical Research Council (MRC) Centre for Regenerative Medicine and UK Dementia Research Institute, University of Edinburgh, Edinburgh EH16 4UU, UK. [2]Institute of Cardiovascular and Medical Sciences, University of Glasgow, Glasgow G12 8QQ, UK. [3]Centre for Cognitive Ageing and Cognitive Epidemiology and MRC Institute of Genetics and Molecular Medicine, University of Edinburgh, Edinburgh EH4 2LF, UK. [4]Erasmus Medical Centre, 3015 CE Rotterdam, Netherlands. [5]Neurology Working Group of the Cohorts for Heart and Aging Research in Genomic Epidemiology (CHARGE). [6]Institute of Molecular Medicine, University of Texas Health Science Center, Houston, TX 77030, USA. [7]Department of Neurology, Boston University School of Medicine, Boston, MA 02118, USA. [8]Centre for Genomic and Experimental Medicine, University of Edinburgh, Edinburgh EH4 2LF, UK. [9]Academic Neuropathology, Centre for Clinical Brain Sciences, University of Edinburgh, Edinburgh EH16 4SB, UK. [10]Brain Research Imaging Centre, Centre for Clinical Brain Sciences, and UK Dementia Research Institute, University of Edinburgh, Edinburgh EH16 4SB, UK.
*Corresponding author. Email: anna.williams@ed.ac.uk

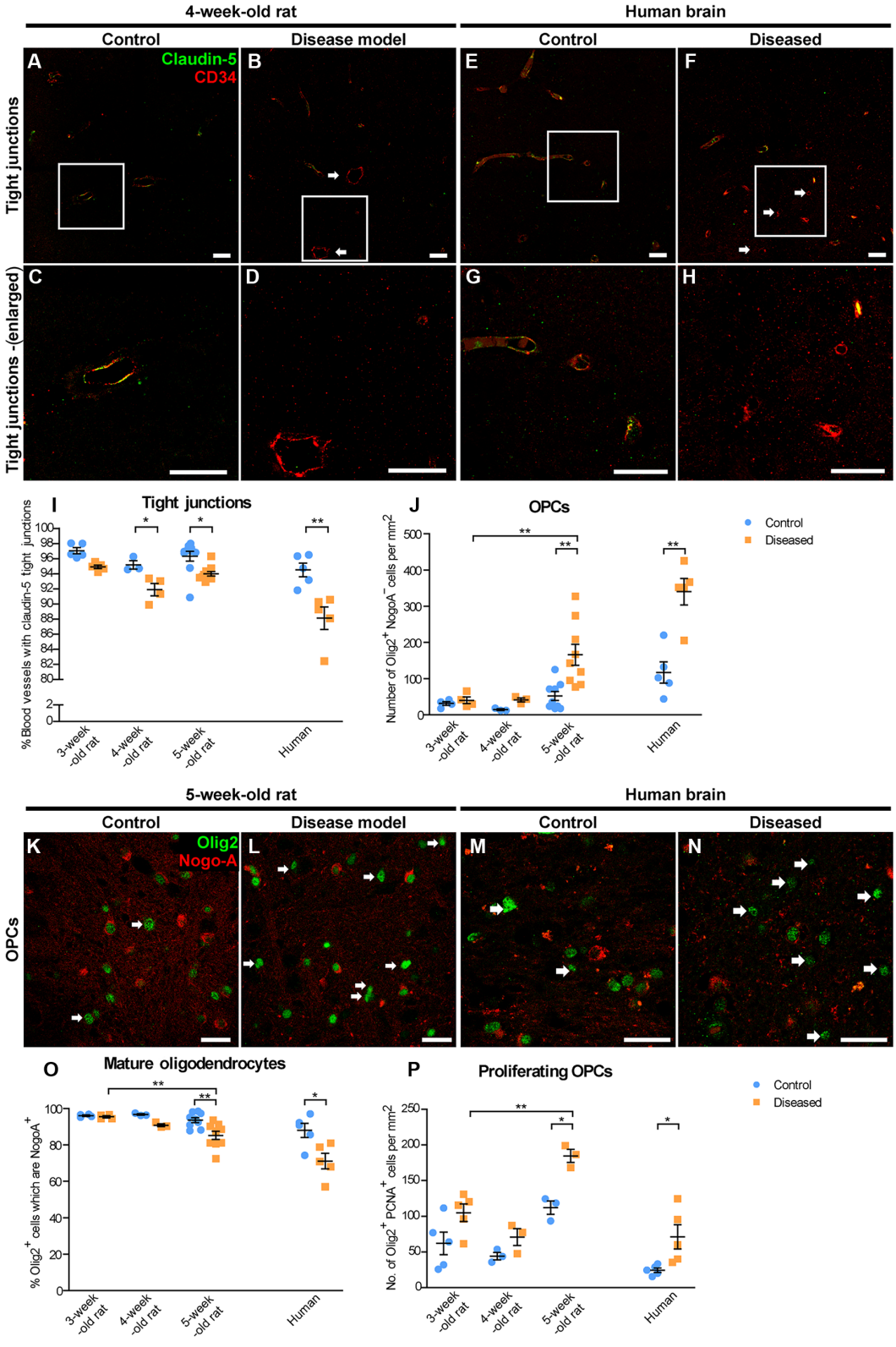

Fig. 1. Pathological changes to the BBB and OPCs in brains of young DM rats and presymptomatic humans. (**A** to **H**) Immunofluorescent images from brain deep white matter and graph (**I**) showing number of blood vessels ($CD34^+$, red) with claudin-5–positive tight junctions (TJs, green) in DM rats (B and D) compared to controls (A and C), as well as in diseased human brains (F and H) compared to controls (E and G). Arrows indicate blood vessels without claudin-5–positive TJs. (C), (D), (G), and (H) show enlarged images of the white boxes in (A), (B), (E), and (F), respectively. (**J** to **O**) Number of OPCs ($Olig2^+$ $Nogo\text{-}A^-$; indicated by arrows) per square millimeter (J and N) and mature oligodendrocytes ($Olig2^+$ $Nogo\text{-}A^+$) (K and O) in DM rats and in diseased human brains compared to controls [Olig2, all oligodendroglia (green); Nogo-A, mature oligodendrocytes (red)]. (**P**) Number of proliferating OPCs ($Olig2^+$ $PCNA^+$) per square millimeter in DM rats and in the diseased human brains compared to controls [mean ± SEM; $*P < 0.05$ and $**P < 0.01$, two-way analysis of variance (ANOVA) with Tukey's post hoc tests; 3 weeks, $n \geq 4$ animals; 4 weeks, $n \geq 3$ animals; 5 weeks, (P) $n = 3$ animals; others, $n = 10$ animals and $n = 5$ humans]. Scale bars, 25 μm. PCNA, proliferating cell nuclear antigen.

DM rats are hypertensive from 6 weeks, show classical SVD pathology from 8 weeks, and suffer strokes from 20 weeks of age (*20*–*24*). As controls, we used the parent strain of the DM rat, Wistar Kyoto (WKY) rats, from a colony maintained in parallel. For human tissue, we used brains obtained from people (aged 24 to 58) who had died suddenly without SVD symptoms but whose brains were found to have early SVD pathology upon postmortem examination (table S1).

BBB changes are found early in a rat SVD model and in humans with presymptomatic SVD

Previous work had found BBB changes in DM rats at 5 weeks of age, predating hypertension (*25*). In deep white matter areas typically affected by SVD pathology, we found that the earliest pathological change seen by immunofluorescence (at 4 weeks of age) was a decrease in the number of blood vessels expressing claudin-5, the key tight junction protein (TJP) of the BBB, indicative of an altered BBB (Fig. 1, A to D and I) (*26*). There was also a trend in the reduction of the absolute amount of claudin-5 protein in DM brain at 5 weeks, although this was not

statistically significant (fig. S1). However, this alteration in claudin-5 expression did not lead to a functional leakage of the BBB to a large dextran tracer in 5-week-old DM rats (fig. S2). In the deep white matter of human brains with early-stage SVD, we found a similar decrease in blood vessels with colocalized claudin-5 expression (Fig. 1, E to I). We found no differences in other components of the BBB, including pericytes, astrocytes, astrocyte end feet, and blood vessel density, between DM and control rats or between the human presymptomatic cases and age-relevant controls (fig. S3).

Oligodendrocyte precursor cells are increased in a rat SVD model and humans with presymptomatic SVD

Subsequent to the BBB changes, we found an increase in oligodendrocyte precursor cells (OPCs) in the deep white matter in the DM rat at 5 weeks of age (more $Olig2^+$ $Nogo\text{-}A^-$ cells; Fig. 1, J to L), as well as in the human presymptomatic cases (Fig. 1, J, M, and N). This increase was due to both a block in OPC differentiation to mature oligodendrocytes (fewer mature $Olig2^+$ $Nogo\text{-}A^+$ oligodendrocytes; Fig. 1O) and an increase in OPC proliferation (Fig. 1P and fig. S4). We also found an increase in the number of macrophages/microglia at 5 weeks of age in DM rats (fig. S5, A, B, and E) and in the human cases (fig. S5, C to E), suggestive of a secondary immune response.

Early changes occur without hypertension or leakage through the BBB

The order of these changes in the DM rat suggests that an early change in the ECs contributes to the later white matter changes and occurs well before the rats become hypertensive. However, the lack of a functional leak in DM rats in vivo at this early time point suggests that early white matter pathology does not result from substances in the blood leaking through an impaired BBB. To confirm this, we cultured brain slices from neonatal DM rats ex vivo for 5 weeks in the absence of blood flow and blood pressure. We observed the same changes as at 5 weeks in vivo: a reduction in claudin-5 protein expression (Fig. 2, A and B), an increase in OPC number (more $Olig2^+$ $Nogo\text{-}A^-$ cells; Fig. 2, C to E), and a reduction in mature oligodendrocytes (fewer $Olig2^+$ $Nogo\text{-}A^+$ oligodendrocytes; Fig. 2F). As these data confirm that neither BBB leakage nor hypertension caused the early myelin pathology in this model, we next considered endothelial dysfunction as a mechanism for the pathology.

DM rats and human SVD brains have dysfunctional ECs

Endothelial dysfunction is commonly defined as a reduction in the bioavailability of nitric oxide (NO) in an EC (*27*). This may be due to either a reduction in NO production by endothelial NO synthase (eNOS) or an increase in NO sequestration by superoxide. At 3 weeks of age, before TJ changes are seen in blood vessels, brains of DM rats already showed reduced eNOS compared to controls (Fig. 2, G and H). Dysfunctional ECs also have a high proliferation rate (*28*, *29*), and we found more proliferating ECs in both 3-week-old DM rat tissue and diseased human brains compared to controls (Fig. 2, I to M). To determine whether this dysfunction was cell-autonomous, we isolated and cultured brain microvascular ECs (BMECs) from neonatal DM and control rats and found that DM cells produced less NO (Fig. 2N). DM BMECs also showed reduced TJ integrity. Control BMECs expressed zonula occludens 1 (ZO-1; a marker of TJs) and claudin-5 (a marker of mature TJs) in their cell membranes. In comparison, DM BMECs expressed ZO-1 normally but showed reduced claudin-5 localization in their membranes (Fig. 2, O to R).

Dysfunctional ECs reduce OPC maturation and increase OPC proliferation

To investigate whether dysfunctional ECs secrete factors that cause the white matter changes in the DM rat, we collected conditioned media (CM) from DM BMECs and added it to in vitro cultures of wild-type OPCs. Treatment with DM BMEC–CM led to a reduction in the maturation of wild-type OPCs (more immature $NG2^+$ OPCs and fewer mature MBP^+ oligodendrocytes; Fig. 3, A to D) and more proliferation (Fig. 3, E to G) compared to wild-type OPCs grown in control BMEC–CM media. Furthermore, ex vivo slice cultures grown in DM BMEC–CM contained more OPCs than slices grown in control BMEC–CM (Fig. 3, H to J). Therefore, secreted factors from DM BMECs affect oligodendroglia biology, blocking OPC maturation and increasing their proliferation. This correlates with the findings seen in tissue sections from young DM rat brains and presymptomatic diseased human brains.

HSP90α secreted by ECs mediates the reduction in OPC maturation

To identify these soluble factors secreted from DM BMECs, we used a forward-phase antibody microarray with >1300 antibodies against select proteins. One protein expressed more in DM compared to control BMEC–CM was heat shock protein 90α (HSP90α; fig. S6), a chaperone protein highly expressed in all brain cell types. We confirmed increased protein in DM BMEC–CM by Western blot (Fig. 3, K and L) and saw a trend in an increase on enzyme-linked immunosorbent assay (ELISA) ($P = 0.05$; Fig. 3M). Treatment of OPCs with recombinant HSP90α (rHSP90α) decreased OPC maturation (more immature $NG2^+$ OPCs and fewer mature MBP^+ oligodendrocytes; Fig. 3, N to Q), mirroring the effect seen with DM BMEC–CM, but had no effect on OPC proliferation compared to controls (fig. S7, A to C). A blocking antibody specific to HSP90α abrogated the DM BMEC–CM–induced maturation defects (Fig. 3, R to V), but again, OPC proliferation was unchanged (fig. S7, D to G). These data show that HSP90α secreted by DM BMECs causes the block in maturation of OPCs but is not responsible for the proliferation effect. Furthermore, we found more of the cleaved secreted form of HSP90α (*30*) in DM rat brains (Fig. 3, W and X) and in some diseased human brains (Fig. 3, W and Y), suggesting that a similar mechanism downstream of endothelial dysfunction also occurs in human SVD.

Drugs that ameliorate endothelial dysfunction reverse OPC changes in vivo

We next investigated whether reducing endothelial dysfunction improves white matter pathology in vivo. We treated DM rats with the following drugs reported to reduce endothelial dysfunction: simvastatin, a cholesterol-lowering drug; perindopril, an angiotensin-converting enzyme inhibitor (ACEI); or cilostazol, a phosphodiesterase inhibitor (*31*–*34*). We dosed animals from 5 weeks old, a time point at which both endothelial and OPC pathologies are present, to adulthood at 12 weeks old (Fig. 4A). These animals were compared to untreated WKY rats, untreated DM rats, and animals treated with a combination drug [hydralazine and hydrochlorothiazide (H+H)] that lowers blood pressure but does not alter endothelial dysfunction, as a control for the blood pressure reduction expected with perindopril (Fig. 4B and table S2). Blood pressures were monitored weekly and increased in all rats over time (as expected as they mature to adulthood) (*35*) but were clustered into two groups: one with high blood pressure (untreated

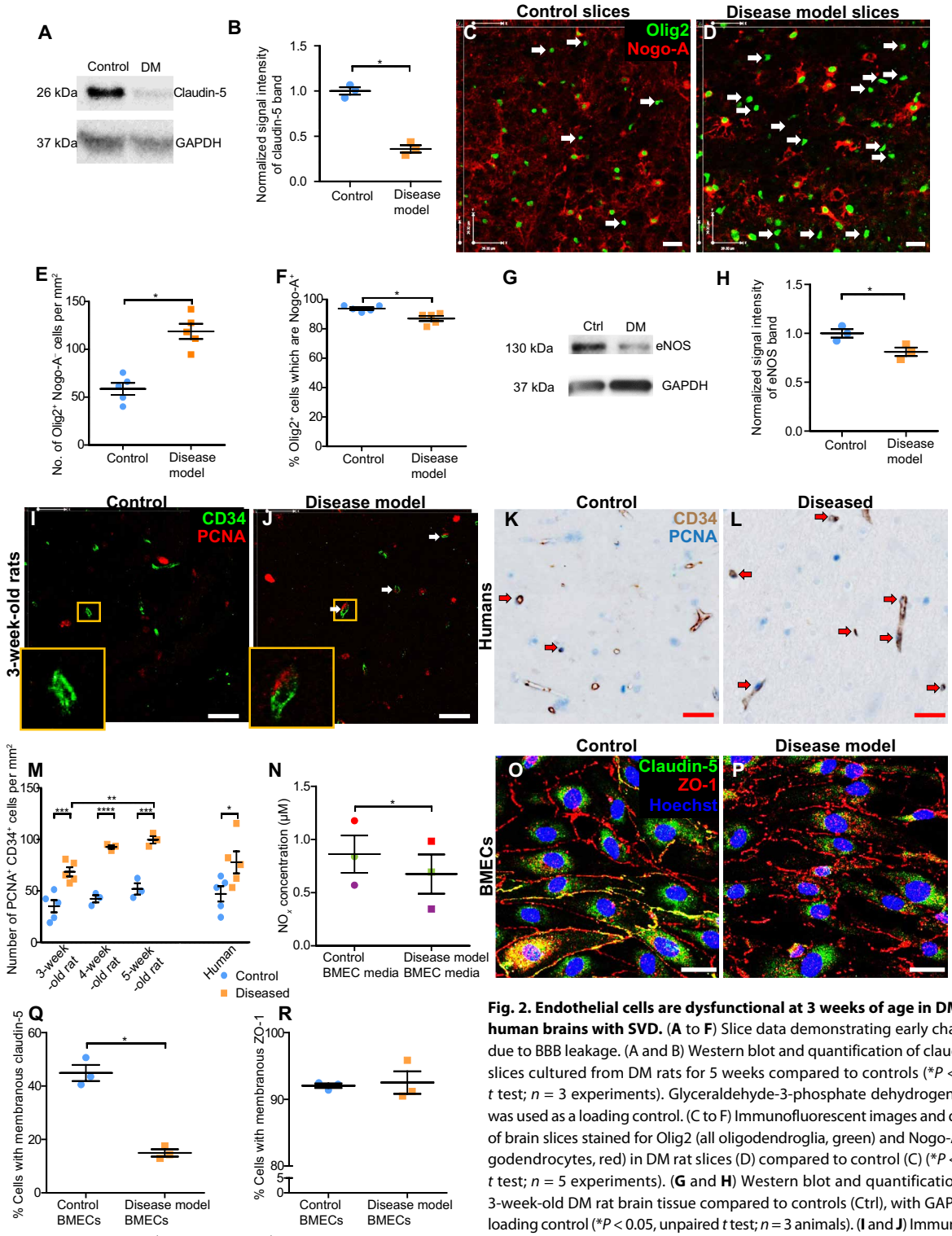

Fig. 2. Endothelial cells are dysfunctional at 3 weeks of age in DM rats and in human brains with SVD. (**A** to **F**) Slice data demonstrating early changes are not due to BBB leakage. (A and B) Western blot and quantification of claudin-5 in brain slices cultured from DM rats for 5 weeks compared to controls (*$P < 0.05$, paired *t* test; $n = 3$ experiments). Glyceraldehyde-3-phosphate dehydrogenase (GAPDH) was used as a loading control. (C to F) Immunofluorescent images and quantification of brain slices stained for Olig2 (all oligodendroglia, green) and Nogo-A (mature oligodendrocytes, red) in DM rat slices (D) compared to control (C) (*$P < 0.05$, paired *t* test; $n = 5$ experiments). (**G** and **H**) Western blot and quantification of eNOS in 3-week-old DM rat brain tissue compared to controls (Ctrl), with GAPDH used as a loading control (*$P < 0.05$, unpaired *t* test; $n = 3$ animals). (**I** and **J**) Immunofluorescent images showing proliferating ($PCNA^+$, red) ECs ($CD34^+$, green) (indicated by white arrows) in the deep white matter of brains from 3-week-old control (I) and DM rats (J). Enlargements of boxed areas are shown. (**K** and **L**) Colorimetric immunostaining of proliferating ($PCNA^+$, blue) human ECs ($CD34^+$, brown) (indicated by red arrows). (**M**) Quantification of the number of proliferating ECs per square millimeter in DM rat brains and the diseased human brains compared to their controls (mean ± SEM; *$P < 0.05$, **$P < 0.01$, ***$P < 0.001$, and ****$P < 0.0001$, two-way ANOVA with Tukey's post hoc tests; 3 weeks, $n = 5$ animals; 4 and 5 weeks, $n = 3$ animals and $n = 5$ humans). (**N**) Assay of nitrates and nitrites (NO_x) as a proxy for cell production of NO in the media of BMECs isolated from DM rats compared to controls. Each color represents a different paired repeat (mean ± SEM; *$P < 0.05$, paired *t* test; $n = 3$ BMEC preparations from different litters). (**O** and **P**) Immunofluorescent staining showing claudin-5 (mature TJP, green) and ZO-1 (immature TJP, red) in BMEC cultures isolated from control (O) and DM (P) rats (Hoechst, blue), quantified in (**Q**) and (**R**) (*$P < 0.05$, paired *t* test; $n = 3$ BMEC preparations from different litters). Scale bars, 25 μm.

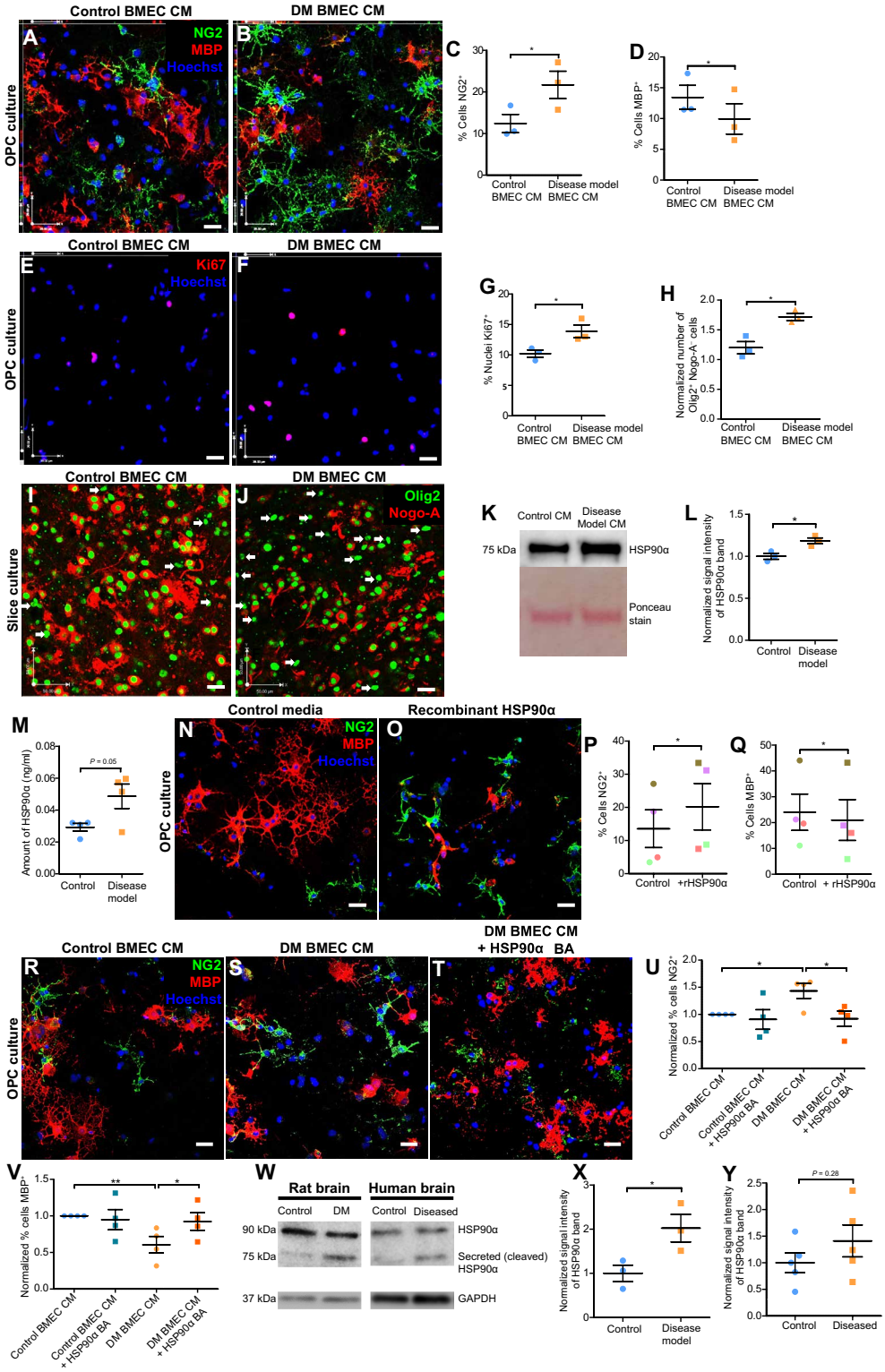

Fig. 3. HSP90α produced by BMECs reduces OPC maturation. (**A** and **B**) Immunofluorescent images showing OPCs ($NG2^+$, green) and MBP^+ mature oligodendrocytes (red) in cultures grown in DM (B) compared to control (A) BMEC–CM (Hoechst, blue) [$^*P < 0.05$, paired *t* test; $n = 3$ experiments, quantified in (**C**) and (**D**)]. (**E** and **F**) Proliferating Ki67-expressing cells (red) in cultures of OPCs grown in DM (F) compared to control (E) BMEC CM (Hoechst, blue) [$^*P < 0.05$, paired *t* test; $n = 3$ experiments, quantified in (**G**)]. (**H** to **J**) OPCs [$Olig2^+$ (all oligodendroglia, green) $Nogo\text{-}A^-$ (mature oligodendrocytes, red), arrows indicating $Olig2^+$ $NogoA^-$ OPCs] in wild-type brain slices grown in culture for 5 weeks in DM BMEC CM (J) compared to control CM (I) [quantified in (H) normalized to slices grown in unconditioned media; $^*P < 0.05$, paired *t* test; $n = 3$ experiments]. (**K**) Western blot for HSP90α in CM from DM BMECs compared to controls ($^*P < 0.05$, paired *t* test; $n = 3$ experiments, quantified in (**L**)], including Ponceau stain of the membrane showing total protein used as a loading control, with prominent band of bovine serum albumin. (**M**) ELISA for HSP90α in CM from DM BMECs compared to controls ($P = 0.05$, *t* test; $n = 4$ experiments). (**N** to **Q**) Effect of addition of recombinant (r) HSP90α on maturation of wild-type OPCs in culture (immature $NG2^+$ OPCs, green; mature MBP^+ oligodendrocytes, red; Hoechst, blue) [quantified in (P) and (Q) with each color representing a different paired repeat; $^*P < 0.05$, paired *t* test; $n = 4$ experiments]. (**R** to **V**) Effect of addition of HSP90α blocking antibody (BA) on OPC cultures grown in DM CM (immature $NG2^+$ OPCs, green; mature MBP^+ oligodendrocytes, red; Hoechst, blue). (U and V) Quantification of the percentage of $NG2^+$ cells is normalized to control CM (such that 1 = an average of 23% $NG2^+$ cells) and quantification of the percentage of MBP^+ cells is normalized to control CM (such that 1 = an average of 15% MBP^+ cells) (mean ± SEM; $^*P < 0.05$ and $^{**}P < 0.01$, one-way repeated measures ANOVA with Bonferroni post hoc tests; $n = 4$ separate experiments with cells from different litters). (**W**) Western blot showing full-length and cleaved, secreted forms of HSP90α (with GAPDH used as a loading control) in rat and human control and diseased brains [$^*P < 0.05$, unpaired *t* test; $n = 3$ rats, each group quantified in (**X**); $P = 0.28$, unpaired *t* test; $n = 5$ humans, each group quantified in (**Y**)]. Scale bars, 25 μm.

DM rats and rats treated with simvastatin or cilostazol) and the other with normal blood pressure (DM rats treated with the antihypertensives perindopril or H+H and untreated WKY rats; Fig. 4C).

At 12 weeks, we examined the brains for signs of endothelial dysfunction and white matter changes. Simvastatin and perindopril significantly reduced EC proliferation ($P < 0.001$ for both; Fig. 4, D, E, and L) and significantly increased mature TJs in DM rats ($P < 0.05$ for both; Fig. 4, F, G, and M), confirming that these drugs improve endothelial dysfunction. Cilostazol showed trend effects only in the same direction. Simvastatin, perindopril, and cilostazol reversed the

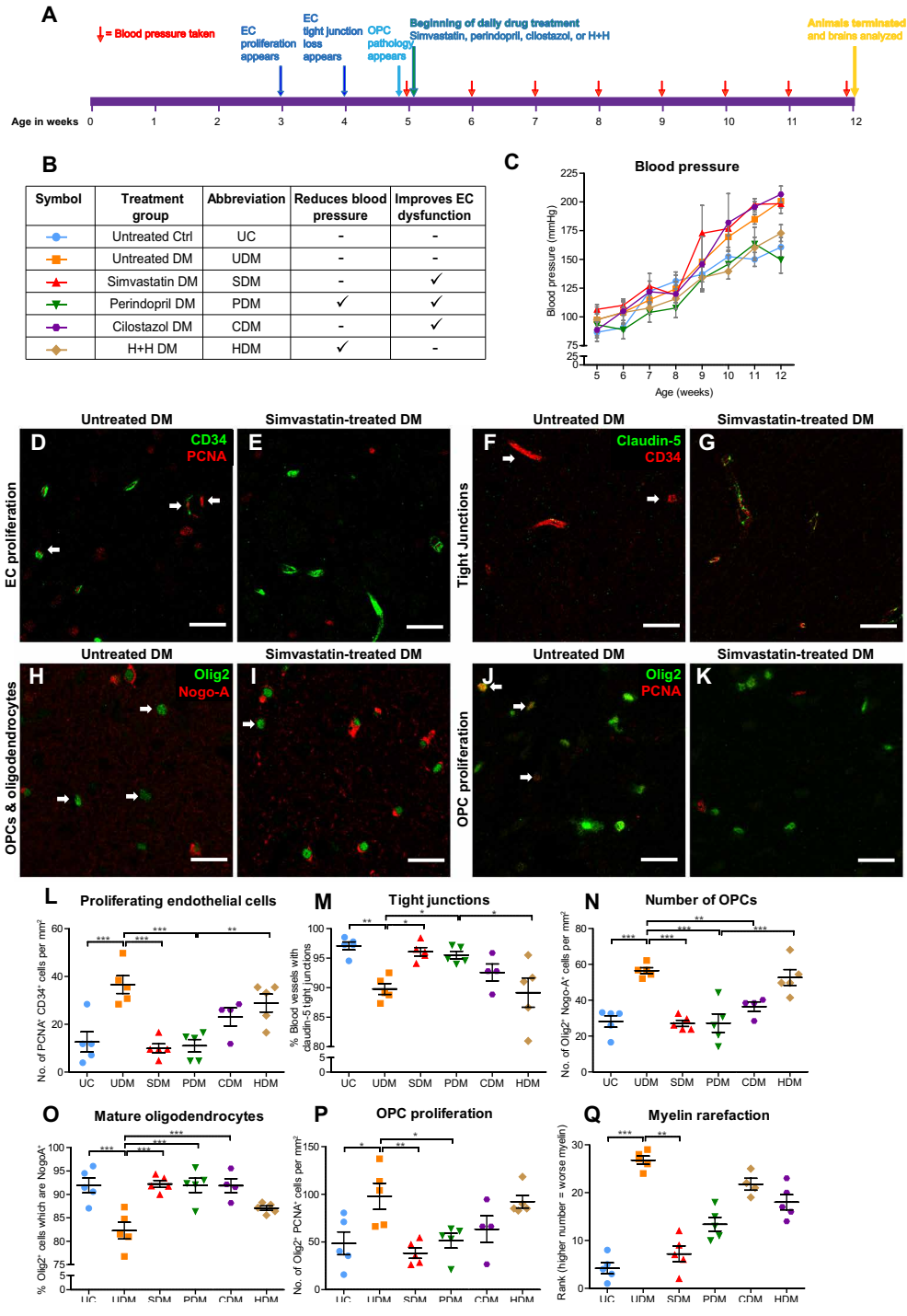

Symbol	Treatment group	Abbreviation	Reduces blood pressure	Improves EC dysfunction
	Untreated Ctrl	UC	-	-
	Untreated DM	UDM	-	-
	Simvastatin DM	SDM	-	✓
	Perindopril DM	PDM	✓	✓
	Cilostazol DM	CDM	-	✓
	H+H DM	HDM	✓	-

Fig. 4. Drugs that reduce EC dysfunction also reduce white matter vulnerability. (**A**) Timeline of drug trial showing the ages at which pathologies appear, the timing of blood pressure measurements, and the beginning and end of treatment. (**B**) Table of treatment groups and effects. All drugs were administered daily through an oral route at the following concentrations: simvastatin, 2 mg/kg; perindopril, 2 mg/kg; cilostazol, 60 mg/kg; and H+H, 16 mg/kg. (**C**) Blood pressure readings over the experiment. (**D** to **K**) Immunofluorescence images showing the effect of simvastatin on EC proliferation, mature TJs, OPC and oligodendrocyte numbers, and OPC proliferation, with quantification in graphs (**L** to **P**). (**Q**) Blinded ranking of myelin rarefaction on Luxol blue/cresyl violet–stained brain sections [mean ± SEM; $*P < 0.05$, $**P < 0.01$, and $***P < 0.001$, (L to P) one-way ANOVA with Bonferroni post hoc tests, and (Q) Kruskal-Wallis test with Dunn's post hoc tests; cilostazol, $n = 4$; others, $n = 5$ animals per treatment group]. Scale bars, 25 μm.

increase in OPCs seen in untreated DM rats ($P < 0.001$, $P < 0.001$, and $P < 0.01$, respectively; Fig. 4, H, I, and N). In the case of simvastatin and perindopril, this is by both reducing the OPC differentiation block ($P < 0.001$ for both; Fig. 4O) and reducing OPC proliferation ($P < 0.01$ for simvastatin and $P < 0.05$ for perindopril; Fig. 4, J, K, and P). Cilostazol only showed a significant increase in mature oligodendrocytes ($P < 0.001$; Fig. 4P). Furthermore, blinded ranking of the quality of myelin in the deep white matter areas showed a pattern of less myelin rarefaction in DM rats treated with drugs reducing EC dysfunction, with a significant reduction for simvastatin ($P < 0.01$; Fig. 4Q). These data demonstrate that improving endothelial dysfunction reverses the oligodendroglial changes in DM rats in vivo, further demonstrating that these are secondary to endothelial dysfunction. These drugs act via different pharmacological pathways, suggesting that endothelial dysfunction reversal itself is the key therapeutic mechanism. This effect is also independent of blood pressure, because normotensive DM rats treated with H+H showed little improvement, and hypertensive DM rats treated with simvastatin and cilostazol showed significant improvements in pathology.

DM rats have a homozygous deletion in *Atp11b*

We next sought to identify the cause of the endothelial dysfunction in our inbred DM rats. We reanalyzed published genomic array sequencing data of the DM rat (SHRSP), the spontaneously hypertensive rat (SHR, which is its closest related strain and develops hypertension but does not show signs of SVD or stroke), and the control strain (WKY) (*36*). As a first-pass analysis, we examined the lists of frameshift mutations and single-nucleotide variants that introduce stop codons because these would be expected to lead to a truncated protein. We selected genes with homozygous mutations occurring in SHRSP but not in SHR, with the assumption that genes mutated in both contribute to the hypertensive phenotype common to both strains, not to the SVD phenotype unique to SHRSP. We then filtered this

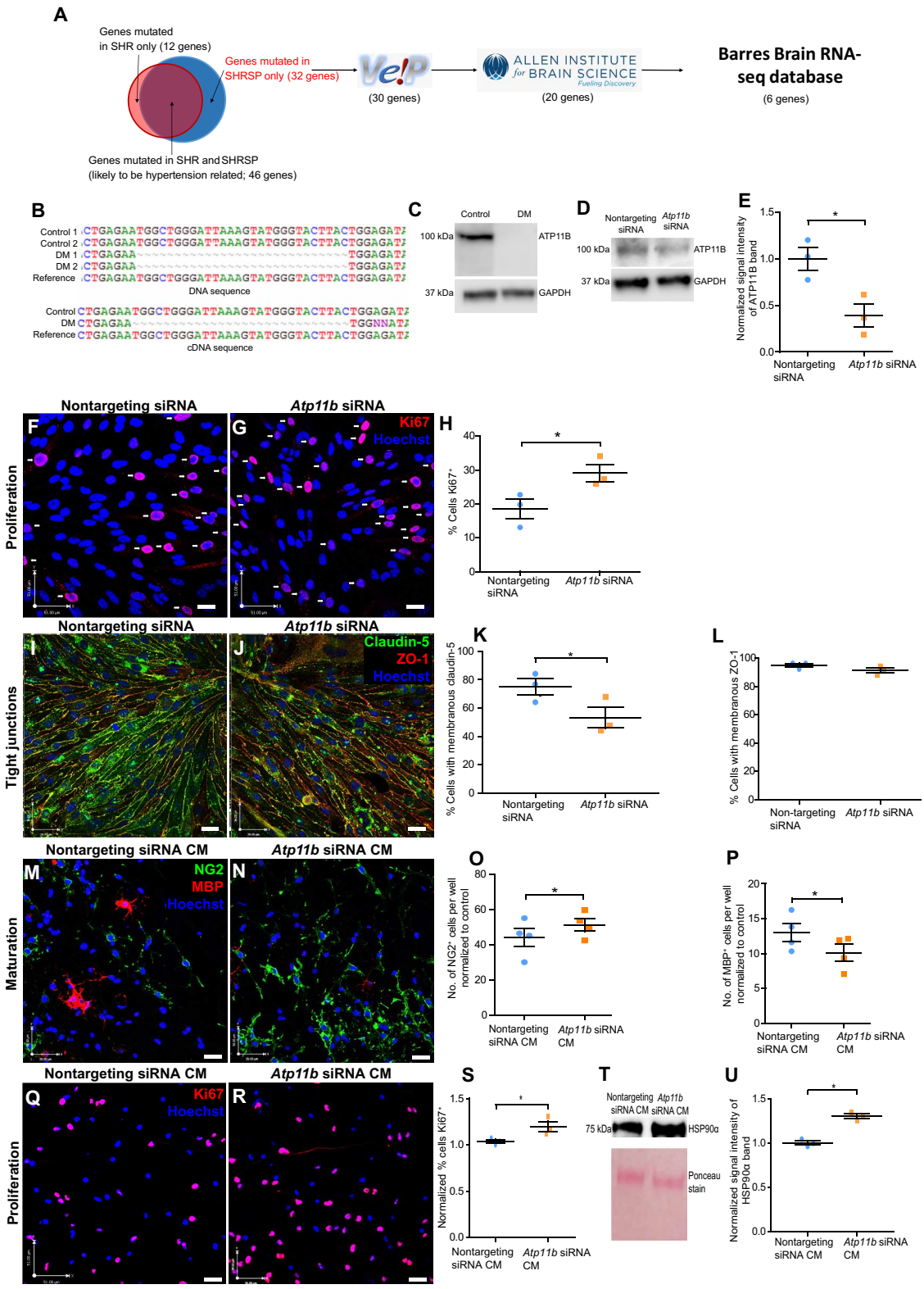

Fig. 5. *Atp11b* is mutated in DM rats and leads to dysfunctional ECs. (**A**) Filtering strategy: Venn diagram with overlap of genes with frameshift or stop-gain mutations in the SHRSP and the SHR. Mutations unique to SHRSP were filtered first using Variant Effect Predictor (Ve!P) tool from Ensembl (*37*) to select those predicted to lead to truncated proteins, then with the Allen Brain Atlas (*38*) to select genes expressed in the brain, and finally with the Barres Brain RNA-seq database (*39*) to select genes expressed in brain ECs. (**B**) DNA sequence showing the 28–base pair deletion in the *Atp11b* gene and corresponding complementary DNA (cDNA). (**C**) Western blot with complete loss of ATP11B in DM rat brains compared to controls using an N-terminal antibody. (**D**) Western blot of knockdown of ATP11B in bEND.3 cells treated with *Atp11b* siRNA (*Atp11b*-KD) compared with nontargeting siRNA (control) [$^*P < 0.05$, paired *t* test; $n = 3$ experiments, quantified in (**E**) with GAPDH used as a loading control]. (**F** and **G**) Immunofluorescent images showing proliferation (Hoechst, blue; Ki67$^+$ nuclei, magenta-white arrows) in *Atp11b*-KD bEND.3 cells (G) compared to controls (F) [quantified in (**H**); $^*P < 0.05$, paired *t* test; $n = 3$ experiments] (Hoechst, blue). (**I** to **L**) Immunofluorescent images staining for claudin-5 (mature TJP, green) compared to ZO-1 (immature TJP, red) in *Atp11b*-KD bEND. 3 cells (J) compared to controls (I) [quantified in (K) and (L); $^*P < 0.05$, paired *t* test; $n = 3$ experiments] (Hoechst, blue). (**M** to **P**) Differentiation of OPCs (NG2$^+$ OPCs, green; mature MBP$^+$ oligodendrocytes, red; Hoechst, blue) cultured in either CM from *Atp11b*-KD bEND.3 cells (N) or control cells (M) [quantified in (O) and (P); $^*P < 0.05$, paired *t* test; $n = 4$ experiments]. (**Q** to **S**) Proliferation (Ki67$^+$, red) of OPCs cultured in CM from *Atp11b*-KD bEND.3 cells (R) compared to controls (Q), quantified in (S) (Hoechst, blue) ($^*P < 0.05$, paired *t* test; $n = 3$ experiments). (**T**) Western blot of HSP90α in CM from *Atp11b*-KD bEND.3 cells compared to controls [quantified in (**U**); $^*P < 0.05$, paired *t* test; $n = 3$ experiments], including Ponceau stain of the membrane showing the total protein (prominent band is bovine serum albumin) used as a loading control. Scale bar, 25 μm.

resulting list of 32 genes further (Fig. 5A) using Ensembl's Variant Effect Predictor tool (*37*) to select mutations resulting in a truncated protein, the Allen Brain Atlas (*38*) to select only those genes expressed in the brain, and the Barres Brain RNA-seq database (*39*) to select genes expressed in brain ECs, because our earlier results demonstrated that the mutation that causes endothelial dysfunction is cell-autonomous. This reduced the list to six genes. Using Sanger sequencing, only one gene was confirmed to have the predicted mutation present in an exon (hence coding and leading to a truncated protein): *Atp11b* (Fig. 5B). By Western blot, we showed that this mutation causes a total loss of ATP11B protein rather than the predicted truncated protein (Fig. 5C).

Knockdown of *Atp11b* in ECs phenocopies DM BMECs

To investigate whether deletion of *Atp11b* causes the endothelial dysfunction observed in our DM rats, we knocked down the gene using small interfering RNA (siRNA) in an EC line (bEND.3), achieving a 61 ± 20% knockdown (KD) of protein (Fig. 5, D and E). *Atp11b*-KD bEND.3 cells showed signs of endothelial dysfunction, with a higher proliferation rate (Fig. 5, F to H) and formation of less mature TJs (Fig. 5, I to L) than cells treated with nontargeting siRNA. Treatment of OPCs with CM collected from *Atp11b*-KD bEND.3 cells caused a block in OPC maturation (more immature $NG2^+$ OPCs and fewer mature MBP^+ oligodendrocytes; Fig. 5, M to P) and increased proliferation (Fig. 5, Q to S). Similarly, CM from human ECs treated with siRNAs to knockdown *ATP11B* led to a block in rat OPC maturation (more $NG2^+$ OPCs and fewer mature MBP^+ oligodendrocytes, proportional to amount of knockdown; fig. S8). Notably, the commercial human cerebral EC lines HBEC5i and hCMEC/d3 did not express endothelial markers and therefore were not used (fig. S9). Furthermore, *Atp11b*-KD bEND. 3 cells secreted more HSP90α compared to those treated with nontargeting siRNA (Fig. 5, T and U), linking the upstream and downstream pathways and suggesting a similar mechanism of action to DM BMECs.

A single-nucleotide polymorphism in *ATP11B* is associated with WMH in humans

To determine whether *ATP11B* is relevant to SVD in humans, we obtained summary data from a previous study, which investigated the genome-wide association of single-nucleotide polymorphisms (SNPs) with WMH burden assessed by MRI (*40*). This study included 17,936 individuals of European descent from 29 population-based cohorts, as part of the Cohorts for Heart and Aging Research in Genomic Epidemiology (CHARGE) consortium (www.chargeconsortium.com). SNPs were imputed from the 1000 Genomes Project reference, and WMH burden was quantified on MRI by either automated segmentation or a visual rating scale. We looked at 304 SNPs within *ATP11B* and found seven SNPs, which were significantly associated with WMH ($P < 0.05$; fig. S10). After correcting for multiple testing, using spectral decomposition to determine the number of independent SNPs tested using the 1000 Genomes Project reference as a measure of linkage disequilibrium (*41*), we found one intronic SNP, which was associated with WMH burden: rs148771930 ($P = 0.00025$).

We used the Genotype-Tissue Expression Portal (GTEx) (www.gtexportal.org) to try to identify expression quantitative trait loci associated with this SNP, but none was identified. We also interrogated RegulomeDB database 46 (www.regulomedb.org/) to identify regulatory DNA elements in noncoding and intergenic regions of the genome in normal cell lines and tissues. Minimal binding evidence was identified (RegulomeDB score = 6), but this included a position weight matrix motif and evidence of histone modifications, suggesting that the SNP may be involved in gene regulation. Although the functional effect of this SNP is not clear, its association with WMH in this data set suggests that *ATP11B* may also be important in the pathogenesis of the human disease. A summary of our model is shown in fig. S11.

DISCUSSION

Here, we demonstrated that endothelial dysfunction is an early precipitant of disease development in a rat model of SVD and a sample of humans with sporadic SVD. We identified a deletion in *Atp11b* and loss of ATP11B protein that cause endothelial dysfunction, with abnormalities of the BBB TJs, increased EC proliferation, and reduction in eNOS and NO. This dysfunction led to secretion of factors, including HSP90α, which blocked the maturation of OPCs into myelinating oligodendrocytes, consistent with the impairment of myelination and inherent vulnerability of white matter to damage seen in adult humans with SVD (*42*). We also demonstrated therapeutic reversal of endothelial dysfunction and associated reduction in white matter vulnerability. The early reduction of the BBB TJ markers but lack of tracer leakage (along with the brain slice culture experiments) showed that leakage of substances through the BBB is not important for initial SVD pathology in our model. However, it is highly likely that BBB leakage is important for later worsening of pathology, because fibrinogen is found around the blood vessels both in late human disease and in the rat SVD model.

There are many possible upstream causes of endothelial dysfunction in SVD, both environmental and genetic. The common environmental risk factors for SVD, such as hypertension, smoking, and diabetes, can induce endothelial dysfunction (*43*–*45*), reconciling the epidemiological associations of SVD. SVD patients have elevated plasma concentrations of soluble biomarkers of endothelial dysfunction, such as intercellular adhesion molecule–1 (*46*), and impaired vasodilation in response to vasoactive challenges (*47*). Animal models of monogenic forms of SVD (such as cerebral autosomal dominant arteriopathy with subcortical infarcts and leukoencephalopathy and *COL4A1* mutations) show reduced vascular reactivity, a sign of endothelial dysfunction (*48*, *49*). Genetic polymorphisms in the gene coding for eNOS, which reduce eNOS activity, are associated with SVD (*50*, *51*).

We found a mutation in *Atp11b* as an upstream cause of endothelial dysfunction in the DM rat. We confirmed that a knockdown of *Atp11b* or *ATP11B* in wild-type rodent and human ECs induced a similar dysfunctional EC phenotype, including an increase in secretion of HSP90α and the secondary effects on OPCs. We also showed that this gene may play a role in human SVD, as an SNP in *ATP11B* was associated with WMH burden. ATP11B is a member of the phospholipid flippase family of proteins, responsible for moving phospholipids from the outer/luminal leaflet of the plasma or organelle membrane to the inner/cytoplasmic leaflet (*52*). ATP11B specifically is involved in vesicular transport from the trans-Golgi network to the plasma membrane (*53*). As the localization of the enzyme eNOS, which shuttles between the Golgi and the plasma membrane, is critical for its ability to produce sufficient NO (*54*), we hypothesize, but have not yet shown, that loss of ATP11B may cause endothelial dysfunction by altering the location and hence the activity of eNOS.

Downstream of endothelial dysfunction, we showed that HSP90α is an important factor secreted from dysfunctional ECs, which mediates

the oligodendroglial maturation defect. The mechanism of action of this OPC maturation block is unknown, but HSP90α, acting through the receptor low-density lipoprotein receptor-related protein 1, can regulate the Akt pathway (*55*), which is key in OPC maturation (*56*, *57*). We also saw increased secretion of HSP90α in brains from humans with sporadic presymptomatic SVD. Therefore, this factor may be downstream of a common pathway of endothelial dysfunction from different causes. Although signaling from OPCs to ECs has been studied previously (*58*, *59*), there is less reported on the effects of ECs on OPCs (*60*–*62*), despite the increasing evidence that SVD patients have dysfunctional ECs and the link between early-life predictors of white matter vulnerability and later SVD (*42*, *63*, *64*).

There is MRI evidence of WMH improving in humans with SVD (*64*). We showed that it was possible to reverse endothelial dysfunction and white matter abnormalities with EC-stabilizing drugs in the early disease state in the rat SVD model. These drugs include statins, which have previously been shown to reduce stroke occurrence in SVD patients but only in patients with elevated cholesterol (*65*). Endothelial dysfunction and OPC changes were also reversed with ACEIs but not with antihypertensives that do not stabilize ECs. Antihypertensives have been extensively tested in clinical trials in human SVD with mixed results (*13*), perhaps secondary to the use of different classes of antihypertensive drugs with different effects on endothelial dysfunction. Trials that exclusively use ACEIs have shown more positive effects on preventing WMH progression in SVD (*66*). Cilostazol acts on ECs through a third mechanism and is currently in early-stage clinical trial for SVD (clinical trial: ISRCTN12580546).

Our study has raised yet unanswered questions. We do not yet know whether this pathology is reversible later in the disease, when leak of blood components through the BBB is also present, and whether these treatments may also have an impact on the clinical behavior of the DM rats. Although this rat model is well recognized as an appropriate model of human SVD, it would be interesting to determine whether a similar mechanism of disease is present in other models including single gene mutation models mirroring human genetic forms of SVD. To determine whether treatment of humans with drugs that stabilize ECs is associated with a better outcome in SVD, it would also be interesting to reassess stroke clinical trial data comparing EC-stabilizing treatment groups with other non–EC-stabilizing antihypertensives.

Here, we show a primary, nonischemic mechanism of endothelial dysfunction in SVD and how this leads to the white matter pathology. We identified an SNP in a gene expressed in ECs in humans that may contribute to vulnerability to SVD. We emphasize that EC function consists of more than just controlling blood flow and that the interactions of ECs and other brain cells—in particular, oligodendroglia—are central to this disease process. We propose that endothelial dysfunction plays a major, causative role in SVD and that reversal of endothelial dysfunction is therapeutic target for effective treatment for this common, disabling, multifactorial disease, with potential for high societal health impact.

MATERIALS AND METHODS

Study design

The overall goal of this study was to determine the mechanism of pathology in cerebral SVD using early presymptomatic human tissue and a rat model of the disease. The use of human tissue for this study was approved by the Medical Research Council Edinburgh Brain and Tissue Bank. This bank has ethical approval to collect tissue for research after informed consent from the next of kin. All animal experiments were carried out in line with UK Home Office guidelines, under project licenses 60/4268 (D.G.), 70/9021 (D.G.), and 60/4524 (A.W.). Treatment groups were randomly assigned, data were analyzed by blinded observers, and biological replicate numbers were stated with each result along with the statistical test used. SHRSP and matched control strain, WKY, were housed at the University of Glasgow. Animals were fed standard chow and housed in line with UK Home Office guidelines. Breeding SHRSP pairs regularly had their blood pressure tested to ensure maintenance of the colony's phenotype. Male animals were exclusively used for both WKY controls and SHRSPs because SHRSP males display a more severe phenotype. Sprague-Dawley rats housed at the University of Edinburgh were used for wild-type OPCs and slice cultures.

Drug study

Animals used in the drug study were individually housed and fed with the drugs mixed in with highly palatable baby food daily from the age of 5 weeks, after pathology first appears, to the age of 12 weeks. Animals were treated in five batches, with each batch containing one animal randomly assigned to each treatment group. Analysis suggested a minimum of five animals per treatment group to detect an effect size of 35% with 80% power (*67*). One animal, which died before the age of 12 weeks without stroke pathology, was not included in the final analysis. Drugs were administered at doses based on previously published data demonstrating their efficacy at either lowering blood pressure or improving endothelial dysfunction when administered orally in rats: simvastatin (2 mg/kg per day; Sigma) (*32*, *33*), perindopril (2 mg/kg per day; Sigma) (*68*), cilostazol (60 mg/kg per day; Sigma) (*69*), and H+H (16 mg/kg per day; Sigma) (*70*) (table S2). Blood pressure was measured before treatment, and weekly after treatment started, by tail-cuff plethysmography. Myelin rarefaction was ranked blind to group from Luxol fast blue/cresyl violet–stained sections.

Human tissue

Human tissue was provided as paraffin-embedded blocks by the Medical Research Council (MRC) Edinburgh Sudden Death Brain Bank. All blocks were from the deep white matter of patients who died suddenly without clinical signs of SVD. Five blocks were chosen from people who had histopathological signs of SVD upon postmortem examination by a neuropathologist (C.S.) and five matched controls were chosen from people with no postmortem signs of SVD [age: control, 46 ± 16 (mean ± SD) and SVD, 49 ± 14; postmortem interval: control, 60 ± 20 hours and SVD, 58 ± 25 hours; percentage male: control, 100% and SVD, 60%]. Full details of the human tissue, including histopathological signs of SVD, are provided in table S1. Unique identifying numbers (MRC database numbers) are listed as follows: SD015/08 (BBN2434), SD021/08 (BBN2440), SD034/08 (BBN2453), SD014/09 (BBN2473), SD010/10 (BBN2507), SD019/08 (BBN2438), SD020/08 (BBN2439), SD022/08 (BBN2481), SD023/08 (BBN2442), and SD031/08 (BBN2450).

Statistical analysis

Graphs were produced, and statistics were calculated using GraphPad Prism software. Data are presented as means ± SEM, comparing at least three biological repeats each time. Numbers and type of biological repeats were stated in each graphical figure legend.

For in vitro studies, an experiment was defined as using cells or slices prepared at different times from different animals or passages. For comparisons between two groups, significance was determined using a two-tailed Student's *t* test, either paired (for in vitro experiments where the control and experimental conditions were run in parallel for each biological repeat) or unpaired. For experiments with multiple comparisons, a one-way or two-way ANOVA was used as appropriate (repeated measures for in vitro experiments), with post hoc Bonferroni or Tukey's tests to determine significance between groups. Statistical significance was defined as $P < 0.05$.

SUPPLEMENTARY MATERIALS

www.sciencetranslationalmedicine.org/cgi/content/full/10/448/eaam9507/DC1
Materials and Methods
Fig. S1. Lower claudin-5 protein in brains of DM rats.
Fig. S2. No leakage of a large dextran tracer indicates normal vascular integrity in 5-week-old DM rats.
Fig. S3. No difference in astrocytes or pericytes.
Fig. S4. Increased number of OPCs due to increased proliferation in DM rats and diseased human brains.
Fig. S5. Brains of young, prehypertensive DM rats and presymptomatic humans show increased numbers of microglia/macrophages.
Fig. S6. More HSP90α is secreted by BMECs isolated from DM rats.
Fig. S7. Addition of rHSP90α or use of blocking antibodies to HSP90α has no effect on OPC proliferation.
Fig. S8. CM from human ECs treated with *ATP11B* siRNA reduces OPC maturation.
Fig. S9. Human cerebral ECs from the HBEC5i and hCMEC/d3 lines do not express endothelial markers.
Fig. S10. SNPs within *ATP11B* are associated with WMH in the CHARGE consortium data.
Fig. S11. Summary of findings illustrating the central role of endothelial dysfunction in SVD pathology.
Table S1. Summary of human SVD and control postmortem data and pathological characteristics.
Table S2. Summary of treatment groups in drug study.
References (*71*–*77*)

REFERENCES AND NOTES

1. M. M. Esiri, G. K. Wilcock, J. H. Morris, Neuropathological assessment of the lesions of significance in vascular dementia. *J. Neurol. Neurosurg. Psychiatry* **63**, 749–753 (1997).
2. A. Smallwood, A. Oulhaj, C. Joachim, S. Christie, C. Sloan, A. D. Smith, M. Esiri, Cerebral subcortical small vessel disease and its relation to cognition in elderly subjects: A pathological study in the Oxford Project to Investigate Memory and Ageing (OPTIMA) cohort. *Neuropathol. Appl. Neurobiol.* **38**, 337–343 (2012).
3. C. Haffner, R. Malik, M. Dichgans, Genetic factors in cerebral small vessel disease and their impact on stroke and dementia. *J. Cereb. Blood Flow Metab.* **36**, 158–171 (2016).
4. K. F. de Laat, A. M. Tuladhar, A. G. W. van Norden, D. G. Norris, M. P. Zwiers, F.-E. de Leeuw, Loss of white matter integrity is associated with gait disorders in cerebral small vessel disease. *Brain* **134**, 73–83 (2011).
5. N. D. Prins, E. J. van Dijk, T. den Heijer, S. E. Vermeer, J. Jolles, P. J. Koudstaal, A. Hofman, M. M. B. Breteler, Cerebral small-vessel disease and decline in information processing speed, executive function and memory. *Brain* **128**, 2034–2041 (2005).
6. S. Debette, H. S. Markus, The clinical importance of white matter hyperintensities on brain magnetic resonance imaging: Systematic review and meta-analysis. *BMJ* **341**, c3666 (2010).
7. J. M. Wardlaw, E. E. Smith, G. J. Biessels, C. Cordonnier, F. Fazekas, R. Frayne, R. I. Lindley, J. T. O'Brien, F. Barkhof, O. R. Benavente, S. E. Black, C. Brayne, M. Breteler, H. Chabriat, C. Decarli, F.-E. de Leeuw, F. Doubal, M. Duering, N. C. Fox, S. Greenberg, V. Hachinski, I. Kilimann, V. Mok, R. van Oostenbrugge, L. Pantoni, O. Speck, B. C. M. Stephan, S. Teipel, A. Viswanathan, D. Werring, C. Chen, C. Smith, M. van Buchem, B. Norrving, P. B. Gorelick, M. Dichgans; STandards for ReportIng Vascular changes on nEuroimaging (STRIVE v1), Neuroimaging standards for research into small vessel disease and its contribution to ageing and neurodegeneration. *Lancet Neurol.* **12**, 822–838 (2013).
8. E. L. Bailey, C. Smith, C. L. M. Sudlow, J. M. Wardlaw, Pathology of lacunar ischemic stroke in humans—A systematic review. *Brain Pathol.* **22**, 583–591 (2012).
9. A. G. Thrift, J. J. McNeil, A. Forbes, G. A. Donnan, Three important subgroups of hypertensive persons at greater risk of intracerebral hemorrhage. Melbourne Risk Factor Study Group. *Hypertension* **31**, 1223–1229 (1998).
10. W.-S. Ryu, S.-H. Woo, D. Schellingerhout, M. K. Chung, C. K. Kim, M. U. Jang, K.-J. Park, K.-S. Hong, S.-W. Jeong, J.-Y. Na, K.-H. Cho, J.-T. Kim, B. J. Kim, M.-K. Han, J. Lee, J.-K. Cha, D.-H. Kim, S. J. Lee, Y. Ko, Y.-J. Cho, B.-C. Lee, K.-H. Yu, M.-S. Oh, J.-M. Park, K. Kang, K. B. Lee, T. H. Park, J. Lee, H.-K. Choi, K. Lee, H.-J. Bae, D.-E. Kim, Grading and interpretation of white matter hyperintensities using statistical maps. *Stroke* **45**, 3567–3575 (2014).
11. E. J. van Dijk, N. D. Prins, H. A. Vrooman, A. Hofman, P. J. Koudstaal, M. M. B. Breteler, Progression of cerebral small vessel disease in relation to risk factors and cognitive consequences: Rotterdam Scan study. *Stroke* **39**, 2712–2719 (2008).
12. S. E. Vermeer, W. T. Longstreth Jr., P. J. Koudstaal, Silent brain infarcts: A systematic review. *Lancet Neurol.* **6**, 611–619 (2007).
13. P. M. Bath, J. M. Wardlaw, Pharmacological treatment and prevention of cerebral small vessel disease: A review of potential interventions. *Int. J. Stroke* **10**, 469–478 (2015).
14. G. A. Lammie, F. Brannan, J. Slattery, C. Warlow, Nonhypertensive cerebral small-vessel disease. An autopsy study. *Stroke* **28**, 2222–2229 (1997).
15. J. M. Wardlaw, P. A. Sandercock, M. S. Dennis, J. Starr, Is breakdown of the blood–brain barrier responsible for lacunar stroke, leukoaraiosis, and dementia? *Stroke* **34**, 806–812 (2003).
16. A. J. Farrall, J. M. Wardlaw, Blood-brain barrier: Ageing and microvascular disease—Systematic review and meta-analysis. *Neurobiol. Aging* **30**, 337–352 (2009).
17. N. J. Abbott, L. Rönnbäck, E. Hansson, Astrocyte-endothelial interactions at the blood–brain barrier. *Nat. Rev. Neurosci.* **7**, 41–53 (2006).
18. J. M. Wardlaw, S. J. Makin, M. C. Valdés Hernández, P. A. Armitage, A. K. Heye, F. M. Chappell, S. Muñoz-Maniega, E. Sakka, K. Shuler, M. S. Dennis, M. J. Thrippleton, Blood–brain barrier failure as a core mechanism in cerebral small vessel disease and dementia: Evidence from a cohort study. *Alzheimer's Dementia* **13**, 634–643 (2017).
19. A. H. Hainsworth, H. S. Markus, Do in vivo experimental models reflect human cerebral small vessel disease? A systematic review. *J. Cereb. Blood Flow Metab.* **28**, 1877–1891 (2008).
20. E. L. Bailey, C. Smith, C. L. M. Sudlow, J. M. Wardlaw, Is the spontaneously hypertensive stroke prone rat a pertinent model of sub cortical ischemic stroke? A systematic review. *Int. J. Stroke* **6**, 434–444 (2011).
21. Y. Yamori, R. Horie, Developmental course of hypertension and regional cerebral blood flow in stroke-prone spontaneously hypertensive rats. *Stroke* **8**, 456–461 (1977).
22. J.-X. Lin, H. Tomimoto, I. Akiguchi, H. Wakita, H. Shibasaki, R. Horie, White matter lesions and alteration of vascular cell composition in the brain of spontaneously hypertensive rats. *Neuroreport* **12**, 1835–1839 (2001).
23. Y. Yamori, R. Horie, H. Handa, M. Sato, M. Fukase, Pathogenetic similarity of strokes in stroke-prone spontaneously hypertensive rats and humans. *Stroke* **7**, 46–53 (1976).
24. J. A. Gratton, A. Sauter, M. Rudin, K. R. Lees, J. McColl, J. L. Reid, A. F. Dominiczak, I. M. Macrae, Susceptibility to cerebral infarction in the stroke-prone spontaneously hypertensive rat is inherited as a dominant trait. *Stroke* **29**, 690–694 (1998).
25. E. L. Bailey, J. M. Wardlaw, D. Graham, A. F. Dominiczak, C. L. M. Sudlow, C. Smith, Cerebral small vessel endothelial structural changes predate hypertension in stroke-prone spontaneously hypertensive rats: A blinded, controlled immunohistochemical study of 5- to 21-week-old rats. *Neuropathol. Appl. Neurobiol.* **37**, 711–726 (2011).
26. T. Nitta, M. Hata, S. Gotoh, Y. Seo, H. Sasaki, N. Hashimoto, M. Furuse, S. Tsukita, Size-selective loosening of the blood-brain barrier in claudin-5–deficient mice. *J. Cell Biol.* **161**, 653–660 (2003).
27. D. G. Harrison, Cellular and molecular mechanisms of endothelial cell dysfunction. *J. Clin. Invest.* **100**, 2153–2157 (1997).
28. M. Drab, P. Verkade, M. Elger, M. Kasper, M. Lohn, B. Lauterbach, J. Menne, C. Lindschau, F. Mende, F. C. Luft, A. Schedl, H. Haller, T. V. Kurzchalia, Loss of caveolae, vascular dysfunction, and pulmonary defects in caveolin-1 gene-disrupted mice. *Science* **293**, 2449–2452 (2001).
29. G. Rajashekhar, A. Willuweit, C. E. Patterson, P. Sun, A. Hilbig, G. Breier, A. Helisch, M. Clauss, Continuous endothelial cell activation increases angiogenesis: Evidence for the direct role of endothelium linking angiogenesis and inflammation. *J. Vasc. Res.* **43**, 193–204 (2006).
30. X. Wang, X. Song, W. Zhuo, Y. Fu, H. Shi, Y. Liang, M. Tong, G. Chang, Y. Luo, The regulatory mechanism of Hsp90α secretion and its function in tumor malignancy. *Proc. Natl. Acad. Sci. U.S.A.* **106**, 21288–21293 (2009).
31. T. F. Lüscher, Endothelial dysfunction: The role and impact of the renin-angiotensin system. *Heart* **84** (suppl. 1), i20–i22 (2000).
32. M. Alvarez de Sotomayor, C. Pérez-Guerrero, M. D. Herrera, E. Marhuenda, Effects of chronic treatment with simvastatin on endothelial dysfunction in spontaneously hypertensive rats. *J. Hypertens.* **17**, 769–776 (1999).
33. J. Carneado, M. Alvarez de Sotomayor, C. Perez-Guerrero, L. Jimenez, M. D. Herrera, E. Pamies, M. D. V. Martin-Sanz, P. Stiefel, M. Miranda, L. Bravo, E. Marhuenda, Simvastatin improves endothelial function in spontaneously hypertensive rats through a superoxide dismutase mediated antioxidant effect. *J. Hypertens.* **20**, 429–437 (2002).

34. A. Hashimoto, G. Miyakoda, Y. Hirose, T. Mori, Activation of endothelial nitric oxide synthase by cilostazol via a cAMP/protein kinase A- and phosphatidylinositol 3-kinase/Akt-dependent mechanism. *Atherosclerosis* **189**, 350–357 (2006).
35. H. H. C. Koh-Tan, M. Dashti, T. Wang, W. Beattie, J. McClure, B. Young, A. F. Dominiczak, M. W. McBride, D. Graham, Dissecting the genetic components of a quantitative trait locus for blood pressure and renal pathology on rat chromosome 3. *J. Hypertens.* **35**, 319–329 (2017).
36. S. S. Atanur, A. G. Diaz, K. Maratou, A. Sarkis, M. Rotival, L. Game, M. R. Tschannen, P. J. Kaisaki, G. W. Otto, M. C. J. Ma, T. M. Keane, O. Hummel, K. Saar, W. X. Chen, V. Guryev, K. Gopalakrishnan, M. R. Garrett, B. Joe, L. Citterio, G. Bianchi, M. McBride, A. E. Dominiczak, D. J. Adams, T. Serikawa, P. Flicek, E. Cuppen, N. Hubner, E. Petretto, D. Gauguier, A. E. Kwitek, H. Jacob, T. J. Aitman, Genome sequencing reveals loci under artificial selection that underlie disease phenotypes in the laboratory rat. *Cell* **154**, 691–703 (2013).
37. F. Cunningham, M. R. Amode, D. Barrell, K. Beal, K. Billis, S. Brent, D. Carvalho-Silva, P. Clapham, G. Coates, S. Fitzgerald, L. Gil, C. G. Girón, L. Gordon, T. Hourlier, S. E. Hunt, S. H. Janacek, N. Johnson, T. Juettemann, A. K. Kähäri, S. Keenan, F. J. Martin, T. Maurel, W. McLaren, D. N. Murphy, R. Nag, B. Overduin, A. Parker, M. Patricio, E. Perry, M. Pignatelli, H. S. Riat, D. Sheppard, K. Taylor, A. Thormann, A. Vullo, S. P. Wilder, A. Zadissa, B. L. Aken, E. Birney, J. Harrow, R. Kinsella, M. Muffato, M. Ruffier, S. M. J. Searle, G. Spudich, S. J. Trevanion, A. Yates, D. R. Zerbino, P. Flicek, Ensembl 2015. *Nucleic Acids Res.* **43**, D662–D669 (2015).
38. E. S. Lein, M. J. Hawrylycz, N. Ao, M. Ayres, A. Bensinger, A. Bernard, A. F. Boe, M. S. Boguski, K. S. Brockway, E. J. Byrnes, L. Chen, L. Chen, T.-M. Chen, M. C. Chin, J. Chong, B. E. Crook, A. Czaplinska, C. N. Dang, S. Datta, N. R. Dee, A. L. Desaki, T. Desta, E. Diep, T. A. Dolbeare, M. J. Donelan, H.-W. Dong, J. G. Dougherty, B. J. Duncan, A. J. Ebbert, G. Eichele, L. K. Estin, C. Faber, B. A. Facer, R. Fields, S. R. Fischer, T. P. Fliss, C. Frensley, S. N. Gates, K. J. Glattfelder, K. R. Halverson, M. R. Hart, J. G. Hohmann, M. P. Howell, D. P. Jeung, R. A. Johnson, P. T. Karr, R. Kawal, J. M. Kidney, R. H. Knapik, C. L. Kuan, J. H. Lake, A. R. Laramee, K. D. Larsen, C. Lau, T. A. Lemon, A. J. Liang, Y. Liu, L. T. Luong, J. Michaels, J. J. Morgan, R. J. Morgan, M. T. Mortrud, N. F. Mosqueda, L. L. Ng, R. Ng, G. J. Orta, C. C. Overly, T. H. Pak, S. E. Parry, S. D. Pathak, O. C. Pearson, R. B. Puchalski, Z. L. Riley, H. R. Rockett, S. A. Rowland, J. J. Royall, M. J. Ruiz, N. R. Sarno, K. Schaffnit, N. V. Shapovalova, T. Sivisay, C. R. Slaughterbeck, S. C. Smith, K. A. Smith, B. I. Smith, A. J. Sodt, N. N. Stewart, K.-R. Stumpf, S. M. Sunkin, M. Sutram, A. Tam, C. D. Teemer, C. Thaller, C. L. Thompson, L. R. Varnam, A. Visel, R. M. Whitlock, P. E. Wohnoutka, C. K. Wolkey, V. Y. Wong, M. Wood, M. B. Yaylaoglu, R. C. Young, B. L. Youngstrom, X. F. Yuan, B. Zhang, T. A. Zwingman, A. R. Jones, Genome-wide atlas of gene expression in the adult mouse brain. *Nature* **445**, 168–176 (2007).
39. Y. Zhang, K. Chen, S. A. Sloan, M. L. Bennett, A. R. Scholze, S. O'Keeffe, H. P. Phatnani, P. Guarnieri, C. Caneda, N. Ruderisch, S. Deng, S. A. Liddelow, C. Zhang, R. Daneman, T. Maniatis, B. A. Barres, J. Q. Wu, An RNA-sequencing transcriptome and splicing database of glia, neurons, and vascular cells of the cerebral cortex. *J. Neurosci.* **34**, 11929–11947 (2014).
40. B. F. J. Verhaaren, S. Debette, J. C. Bis, J. A. Smith, M. K. Ikram, H. H. Adams, A. H. Beecham, K. B. Rajan, L. M. Lopez, S. Barral, M. A. van Buchem, J. van der Grond, A. V. Smith, K. Hegenscheid, N. T. Aggarwal, M. de Andrade, E. J. Atkinson, M. Beekman, A. S. Beiser, S. H. Blanton, E. Boerwinkle, A. M. Brickman, R. N. Bryan, G. Chauhan, C. P. L. H. Chen, V. Chouraki, A. J. M. de Craen, F. Crivello, I. J. Deary, J. Deelen, P. L. De Jager, C. Dufouil, M. S. V. Elkind, D. A. Evans, P. Freudenberger, R. F. Gottesman, V. Guðnason, M. Habes, S. R. Heckbert, G. Heiss, S. Hilal, E. Hofer, A. Hofman, C. A. Ibrahim-Verbaas, D. S. Knopman, C. E. Lewis, J. Liao, D. C. M. Liewald, M. Luciano, A. van der Lugt, O. O. Martinez, R. Mayeux, B. Mazoyer, M. Nalls, M. Nauck, W. J. Niessen, B. A. Oostra, B. M. Psaty, K. M. Rice, J. I. Rotter, B. von Sarnowski, H. Schmidt, P. J. Schreiner, M. Schuur, S. S. Sidney, S. Sigurdsson, P. E. Slagboom, D. J. M. Stott, J. C. van Swieten, A. Teumer, A. M. Töglhofer, M. Traylor, S. Trompet, S. T. Turner, C. Tzourio, H.-W. Uh, A. G. Uitterlinden, M. W. Vernooij, J. J. Wang, T. Y. Wong, J. M. Wardlaw, B. G. Windham, K. Wittfeld, C. Wolf, C. B. Wright, Q. Yang, W. Zhao, A. Zijdenbos, J. W. Jukema, R. L. Sacco, S. L. R. Kardia, P. Amouyel, T. H. Mosley, W. T. Longstreth Jr., C. C. DeCarli, C. M. van Duijn, R. Schmidt, L. J. Launer, H. J. Grabe, S. S. Seshadri, M. A. Ikram, M. Fornage, Multiethnic genome-wide association study of cerebral white matter hyperintensities on MRI. *Circ. Cardiovasc. Genet.* **8**, 398–409 (2015).
41. D. R. Nyholt, A simple correction for multiple testing for single-nucleotide polymorphisms in linkage disequilibrium with each other. *Am. J. Hum. Genet.* **74**, 765–769 (2004).
42. E. V. Backhouse, C. A. McHutchison, V. Cvoro, S. D. Shenkin, J. M. Wardlaw, Early life risk factors for cerebrovascular disease: A systematic review and meta-analysis. *Neurology* **88**, 976–984 (2017).
43. K. Ozaki, T. Hori, T. Ishibashi, M. Nishio, Y. Aizawa, Effects of chronic cigarette smoking on endothelial function in young men. *J. Cardiol.* **56**, 307–313 (2010).
44. M. T. Johnstone, S. J. Creager, K. M. Scales, J. A. Cusco, B. K. Lee, M. A. Creager, Impaired endothelium-dependent vasodilation in patients with insulin-dependent diabetes mellitus. *Circulation* **88**, 2510–2516 (1993).
45. J. A. Panza, A. A. Quyyumi, J. E. Brush Jr., S. E. Epstein, Abnormal endothelium-dependent vascular relaxation in patients with essential hypertension. *N. Engl. J. Med.* **323**, 22–27 (1990).
46. A. Poggesi, M. Pasi, F. Pescini, L. Pantoni, D. Inzitari, Circulating biologic markers of endothelial dysfunction in cerebral small vessel disease: A review. *J. Cereb. Blood Flow Metab.* **36**, 72–94 (2016).
47. S. F. Stevenson, F. N. Doubal, K. Shuler, J. M. Wardlaw, A systematic review of dynamic cerebral and peripheral endothelial function in lacunar stroke versus controls. *Stroke* **41**, e434–e442 (2010).
48. A. Joutel, M. Monet-Leprêtre, C. Gosele, C. Baron-Menguy, A. Hammes, S. Schmidt, B. Lemaire-Carrette, V. Domenga, A. Schedl, P. Lacombe, N. Hubner, Cerebrovascular dysfunction and microcirculation rarefaction precede white matter lesions in a mouse genetic model of cerebral ischemic small vessel disease. *J. Clin. Invest.* **120**, 433–445 (2010).
49. T. Van Agtmael, M. A. Bailey, U. Schlötzer-Schrehardt, E. Craigie, I. J. Jackson, D. G. Brownstein, I. L. Megson, J. J. Mullins, Col4a1 mutation in mice causes defects in vascular function and low blood pressure associated with reduced red blood cell volume. *Hum. Mol. Genet.* **19**, 1119–1128 (2010).
50. A. Elbaz, O. Poirier, T. Moulin, F. Chédru, F. Cambien, P. Amarenco, Association between the Glu298Asp polymorphism in the endothelial constitutive nitric oxide synthase gene and brain infarction. The GÉNIC Investigators. *Stroke* **31**, 1634–1639 (2000).
51. A. Hassan, K. Gormley, M. O'Sullivan, J. Knight, P. Sham, P. Vallance, J. Bamford, H. Markus, Endothelial nitric oxide gene haplotypes and risk of cerebral small-vessel disease. *Stroke* **35**, 654–659 (2004).
52. X. Tang, M. S. Halleck, R. A. Schlegel, P. Williamson, A subfamily of P-type ATPases with aminophospholipid transporting activity. *Science* **272**, 1495–1497 (1996).
53. M. Moreno-Smith, J. B. Halder, P. S. Meltzer, T. A. Gonda, L. S. Mangala, R. Rupaimoole, C. Lu, A. S. Nagaraja, K. M. Gharpure, Y. Kang, C. Rodriguez-Aguayo, P. E. Vivas-Mejia, B. Zand, R. Schmandt, H. Wang, R. R. Langley, N. B. Jennings, C. Ivan, J. E. Coffin, G. N. Armaiz, J. Bottsford-Miller, S. B. Kim, M. S. Halleck, M. J. C. Hendrix, W. Bornman, M. Bar-Eli, J.-S. Lee, Z. H. Siddik, G. Lopez-Berestein, A. K. Sood, ATP11B mediates platinum resistance in ovarian cancer. *J. Clin. Invest.* **123**, 2119–2130 (2013).
54. Q. Zhang, J. E. Church, D. Jagnandan, J. D. Catravas, W. C. Sessa, D. Fulton, Functional relevance of Golgi- and plasma membrane-localized endothelial NO synthase in reconstituted endothelial cells. *Arterioscler. Thromb. Vasc. Biol.* **26**, 1015–1021 (2006).
55. S. Sato, N. Fujita, T. Tsuruo, Modulation of Akt kinase activity by binding to Hsp90. *Proc. Natl. Acad. Sci. U.S.A.* **97**, 10832–10837 (2000).
56. A. I. Flores, B. S. Mallon, T. Matsui, W. Ogawa, A. Rosenzweig, T. Okamoto, W. B. Macklin, Akt-mediated survival of oligodendrocytes induced by neuregulins. *J. Neurosci.* **20**, 7622–7630 (2000).
57. C. R. Sussman, T. Vartanian, R. H. Miller, The ErbB4 neuregulin receptor mediates suppression of oligodendrocyte maturation. *J. Neurosci.* **25**, 5757–5762 (2005).
58. T. J. Yuen, J. C. Silbereis, A. Griveau, S. M. Chang, R. Daneman, S. P. J. Fancy, H. Zahed, E. Maltepe, D. H. Rowitch, Oligodendrocyte-encoded HIF function couples postnatal myelination and white matter angiogenesis. *Cell* **158**, 383–396 (2014).
59. D. A. Mayes, T. A. Rizvi, H. E. Titus-Mitchell, R. Oberst, G. M. Ciraolo, C. V. Vorhees, A. P. Robinson, S. D. Miller, J. A. Cancelas, A. O. Stemmer-Rachamimov, N. Ratner, Nf1 loss and Ras hyperactivation in oligodendrocytes induce NOS-driven defects in myelin and vasculature. *Cell Rep.* **4**, 1197–1212 (2013).
60. H.-H. Tsai, J. Niu, R. Munji, D. Davalos, J. Chang, H. Zhang, A.-C. Tien, C. J. Kuo, J. R. Chan, R. Daneman, S. P. J. Fancy, Oligodendrocyte precursors migrate along vasculature in the developing nervous system. *Science* **351**, 379–384 (2016).
61. K. Arai, E. H. Lo, An oligovascular niche: Cerebral endothelial cells promote the survival and proliferation of oligodendrocyte precursor cells. *J. Neurosci.* **29**, 4351–4355 (2009).
62. R. M. Rajani, A. Williams, Endothelial cell-oligodendrocyte interactions in small vessel disease and aging. *Clin. Sci.* **131**, 369–379 (2017).
63. M. del C. Valdés Hernandez, T. Booth, C. Murray, A. J. Gow, L. Penke, Z. Morris, S. M. Maniega, N. A. Royle, B. S. Aribisala, M. E. Bastin, J. M. Starr, I. J. Deary, J. M. Wardlaw, Brain white matter damage in aging and cognitive ability in youth and older age. *Neurobiol. Aging* **34**, 2740–2747 (2013).
64. J. M. Wardlaw, M. C. Valdés Hernández, S. Muñoz-Maniega, What are white matter hyperintensities made of? Relevance to vascular cognitive impairment. *J. Am. Heart Assoc.* **4**, e001140 (2015).
65. J. H. Fu, V. Mok, W. Lam, A. Wong, W. Chu, Y. Xiong, P. W. Ng, T. H. Tsoi, V. Yeung, K. S. Wong, Effects of statins on progression of subclinical brain infarct. *Cerebrovasc. Dis.* **30**, 51–56 (2010).
66. C. Dufouil, J. Chalmers, O. Coskun, V. Besançon, M.-G. Bousser, P. Guillon, S. MacMahon, B. Mazoyer, B. Neal, M. Woodward, N. Tzourio-Mazoyer, C. Tzourio; PROGRESS MRI Substudy Investigators, Effects of blood pressure lowering on cerebral white matter hyperintensities in patients with stroke: The PROGRESS (Perindopril Protection Against Recurrent Stroke Study) Magnetic Resonance Imaging Substudy. *Circulation* **112**, 1644–1650 (2005).

67. H. M. Vesterinen, E. S. Sena, C. ffrench-Constant, A. Williams, S. Chandran, M. R. Macleod, Improving the translational hit of experimental treatments in multiple sclerosis. *Mult. Scler.* **16**, 1044–1055 (2010).
68. N. H. Anderson, A. M. Devlin, D. Graham, J. J. Morton, C. A. Hamilton, J. L. Reid, N. J. Schork, A. F. Dominiczak, Telemetry for cardiovascular monitoring in a pharmacological study: New approaches to data analysis. *Hypertension* **33**, 248–255 (1999).
69. H. Edrissi, S. C. Schock, R. Cadonic, A. M. Hakim, C. S. Thompson, Cilostazol reduces blood brain barrier dysfunction, white matter lesion formation and motor deficits following chronic cerebral hypoperfusion. *Brain Res.* **1646**, 494–503 (2016).
70. H. H. C. Koh-Tan, D. Graham, C. A. Hamilton, G. Nicoll, L. Fields, M. W. McBride, B. Young, A. F. Dominiczak, Renal and vascular glutathione S-transferase μ is not affected by pharmacological intervention to reduce systolic blood pressure. *J. Hypertens.* **27**, 1575–1584 (2009).
71. H. Zhang, A. A. Jarjour, A. Boyd, A. Williams, Central nervous system remyelination in culture—A tool for multiple sclerosis research. *Exp. Neurol.* **230**, 138–148 (2011).
72. G. Levi, Nouvelles recherches sur le tissu nerveux cultivé in vitro; Morphologie, croissance et relations réciproques des neurones. *Arch. Biol.* **52**, 133–160 (1941).
73. N. J. Abbott, C. C. Hughes, P. A. Revest, J. Greenwood, Development and characterisation of a rat brain capillary endothelial culture: Towards an in vitro blood-brain barrier. *J. Cell Sci.* **103** (pt. 1), 23–37 (1992).
74. K. D. McCarthy, J. de Vellis, Preparation of separate astroglial and oligodendroglial cell cultures from rat cerebral tissue. *J. Cell Biol.* **85**, 890–902 (1980).
75. W. Li, Y. Li, S. Guan, J. Fan, C.-F. Cheng, A. M. Bright, C. Chinn, M. Chen, D. T. Woodley, Extracellular heat shock protein-90α: Linking hypoxia to skin cell motility and wound healing. *EMBO J.* **26**, 1221–1233 (2007).
76. N. K. Acharya, E. L. Goldwaser, M. M. Forsberg, G. A. Godsey, C. A. Johnson, A. Sarkar, C. DeMarshall, M. C. Kosciuk, J. M. Dash, C. P. Hale, D. M. Leonard, D. M. Appelt, R. G. Nagele, Sevoflurane and isoflurane induce structural changes in brain vascular endothelial cells and increase blood–brain barrier permeability: Possible link to postoperative delirium and cognitive decline. *Brain Res.* **1620**, 29–41 (2015).
77. A. B. Nair, S. Jacob, A simple practice guide for dose conversion between animals and human. *J. Basic Clin. Pharm.* **7**, 27–31 (2016).

Acknowledgments: We thank the MRC Edinburgh Sudden Death Brain Bank for providing human brain tissue and CHARGE consortium for the provision of SNP data. We also thank M. Swire and C. ffrench-Constant for providing us with the bEND.3 cell line, E. Beattie for assistance with in vivo work, B. Vernay and M. Ahmed for help with imaging, and V. Miron for commenting on an earlier draft of the manuscript. **Funding:** This work was supported by the UK Medical Research Council, Alzheimer's Research UK, Fondation Leducq (16 CVD 05), and the British Heart Foundation Centre for Research Excellence (RE/13/5/30177). S.E.H. is supported by the University of Edinburgh Centre for Cognitive Ageing and Cognitive Epidemiology, funded by the MRC and Biotechnology and Biological Sciences Research Council (grant no. MR/K026992/1). **Author contributions:** R.M.R. designed, carried out, and analyzed most of the experiments and wrote the manuscript. S.Q. carried out the human EC work, ELISAs, tracer experiments, and some Western blots. S.R.R. carried out the CM experiments on slices and assisted with the rat sequencing. D.G. and A.F.D. provided the SHRSP and WKY rats, and D.G. carried out the perfusions and assisted with the drug study. B.F.J.V, M.F., and S.S. provided the SNP summary data, and S.E.H. carried out the multiple testing correction. S.S.A. provided advice on reanalysis of the rat gene array data. C.S. and J.M.W co-supervised the project and assisted in study design. J.M.W. initiated the original experiments, added important context, and assisted in data interpretation and editing of the manuscript. A.W. supervised the project and assisted in study design, data interpretation, and writing of the manuscript. All authors assisted with editing of the manuscript. **Competing interests:** The authors declare that they have no competing financial interests. **Data and materials availability:** All relevant data are available in the manuscript and in the Supplementary Materials. Requests for materials should be addressed to A.W. (anna.williams@ed.ac.uk).

Submitted 9 February 2017
Resubmitted 31 January 2018
Accepted 8 June 2018
Published 4 July 2018
10.1126/scitranslmed.aam9507

Citation: R. M. Rajani, S. Quick, S. R. Ruigrok, D. Graham, S. E. Harris, B. F. J. Verhaaren, M. Fornage, S. Seshadri, S. S. Atanur, A. F. Dominiczak, C. Smith, J. M. Wardlaw, A. Williams, Reversal of endothelial dysfunction reduces white matter vulnerability in cerebral small vessel disease in rats. *Sci. Transl. Med.* **10**, eaam9507 (2018).

Science Translational Medicine

Reversal of endothelial dysfunction reduces white matter vulnerability in cerebral small vessel disease in rats

Rikesh M. Rajani, Sophie Quick, Silvie R. Ruigrok, Delyth Graham, Sarah E. Harris, Benjamin F. J. Verhaaren, Myriam Fornage, Sudha Seshadri, Santosh S. Atanur, Anna F. Dominiczak, Colin Smith, Joanna M. Wardlaw and Anna Williams

Sci Transl Med **10**, eaam9507.
DOI: 10.1126/scitranslmed.aam9507

Defeating dysfunction

Cerebral small vessel disease (SVD) affects arterioles in the brain, increasing risk of stroke and causing symptoms of dementia. To understand the link between vascular changes and white matter pathology, Rajani and colleagues studied a rat model of SVD. Vascular tight junctions were impaired in SVD, and dysfunctional endothelial cells prevented oligodendrocyte precursors from maturing into myelinating cells. SVD rats had a mutation in an ATPase, which was also found in SVD human brain tissue. Drugs that stabilized endothelial cells could reverse the white matter abnormalities in early-stage SVD in the rat model, suggesting a potential therapeutic approach.